Assessment of Mechatronic System Performance at an Early Design Stage

Erik Coelingh, *Member, IEEE*, Theo J. A. de Vries, *Member, IEEE*, and Rien Koster

***Abstract*—For conceptual design of electromechanical motion systems, an assessment method is formulated that supports the design of a feasible reference path generator, control system, and electromechanical plant with appropriate sensor locations, in an integrated way. This method is based on a classification of standard transfer functions, plant models, and closed-loop systems. The assessment method can be applied in several ways, depending on the available knowledge about the design problem. In order to illustrate this method, an application to an industrial motion system is described. The assessment method quickly provides insight in the design problem. Furthermore, feasible goals and required design efforts can be estimated at an early stage.**

***Index Terms*—Design, mechatronics, motion control, proportional differential (PD) controllers.**

I. Introduction

During conceptual design of controlled electromechanical motion systems, one has to obtain feasible technical design specifications for the path generator, the control system, and the electromechanical plant with appropriate sensor locations, so that the overall system will perform well. In case a mechatronic design approach is followed, this should be done in an integrated way. That is, the specifications of the subsystems should somehow be balanced in such a way that completing the designs of the subsystems will require about the same design effort. When we want to achieve this aim, we encounter a "chicken-and-egg" difficulty. In order to balance the subsystem specifications, we have to estimate the influence that the controller will have on the system's performance. However, to estimate this, we need to complete a controller design. The methods available for this require both definitive specifications and a definitive model of the electromechanical plant, which are not yet available early in the design process. In this paper, this problem will be addressed, specifically for systems where the task is to position an end effector at a certain location within a limited period.

During conceptual design, the aim is not to complete a final design, but rather to identify the performance-limiting factors of the design proposal(s) and to choose satisfactory specifications for these factors. Experience has taught us that the following factors dominantly determine system performance.

1) *Task specification*: Motion distance, motion time, required positional accuracy after motion time.
2) *Path generator*: Smoothness of the path.
3) *Controller*: Proportional and differential gain.
4) *Plant*: Total mass to be moved, lowest eigenfrequency, location of the position (and velocity) sensor(s).

The dominant plant factors motivate the use of simple fourth-order models, i.e., lumped parameter representations of the dominant dynamic behavior of electromechanical motion systems in terms of one discrete stiffness and the related mass distribution. Such models take only the rigid-body mode and the lowest mode of vibration into account. They are simple and of low-order, have a small number of parameters, and yet competently describe the performance-limiting factor. Hence, they are a good basis to provide reliable estimates of the dominant dynamic behavior and the attainable closed-loop bandwidth. The mass-spring-mass plant is a well-known example, of which the often stated industrial relevance [1], [2] can be understood from the above considerations.

In this paper, a procedure will be given that allows assessing the influence of the above mentioned design factors on the system performance. By means of iterative application of this procedure, the "chicken-and-egg" difficulty of formulating well-balanced subsystem specifications can be solved.

Before formulating the procedure, we start by classifying plant dynamics. First, basic open-loop transfer functions are described in Section II. In Section III, it is shown how these transfer functions are obtained from different physical plant models and sensor locations. In Section IV, a characterization of closed-loop system dynamics follows and in Section V, the method for relating design factors to system performance is described. The resulting assessment procedure is given in Section VI. In Section VII, the assessment procedure is applied to an industrial motion system: the placement module of the Philips Fast Component Mounter. Finally, in Section VIII, the conclusions are presented.

II. Basic Open-Loop Transfer Function Types

We consider plant transfer functions $P(s)$ from the input force u to a measured position y. The mechanical damping in the plant is neglected. In general, damping does not dominate the dynamics of the mechanism and it unnecessarily complicates the considerations that follow here. We also do not explicitly consider the influence of friction, as mechanical friction is difficult to estimate and highly nonlinear [3]; it should preferably be minimized by means of proper mechanical design. In any way, it will usually be impossible to anticipate friction characteristics of a plant during the conceptual design stage.

Manuscript received March 24, 2000. Recommended by Technical Editor B. Ravani.

The authors are with the Drebbel Institute for Mechatronics, Control Laboratory, University of Twente, 7500 AE Enschede, The Netherlands (e-mail: t.j.a.devries@el.utwente.nl; mechatronics@rt.el.utwente.nl).

Publisher Item Identifier 10.1109/TMECH.2002.803630.

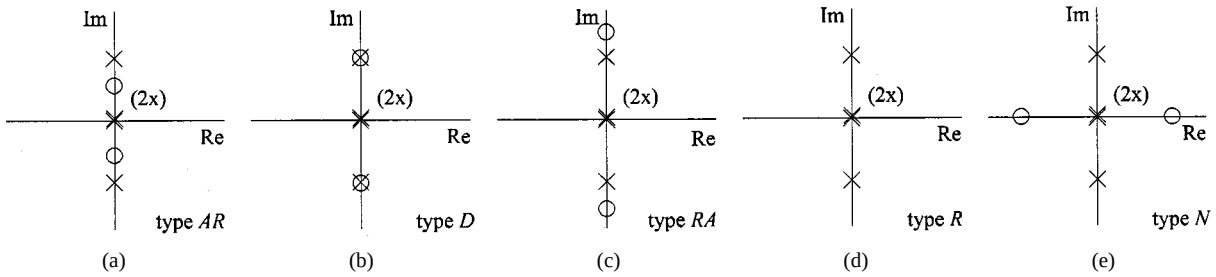

Fig. 1. Pole–zero maps of basic open-loop transfer functions.

The denominator polynomial of $P(s)$ is always the same for a particular dynamic system, but the numerator polynomial depends on the locations of the actuator and the position sensor. For systems with mechanical flexibilities, this dependency is described extensively in [4]. In [5], it is shown how a zero pair moves along the imaginary axis for different locations of the sensor. We will use this phenomenon, which is referred to as *migration of zeros*, to characterize five different *types* of plant transfer functions at an abstract level. This characterization originates from [6] and [7]. We consider the location of the complex conjugate zero pair in the s plane with respect to the complex conjugate pole pair. We will refer to these pairs as the antiresonance frequency $\omega_{\rm ar}$, respectively, the resonance frequency $\omega_{\rm r}$ of a plant transfer function.

A. Type AR: Antiresonance–Resonance

The type *AR* transfer function is

$$P_{AR}(s) = \frac{1}{ms^2} \cdot \frac{s^2 + {\omega_{\rm ar}}^2}{s^2 + {\omega_{\rm r}}^2} \cdot \frac{{\omega_{\rm r}}^2}{{\omega_{\rm ar}}^2}, \qquad \omega_{\rm ar} < \omega_{\rm r} \quad (1)$$

where m is the total mass to be moved. The pole–zero map is shown in Fig. 1(a). Note that the antiresonance frequency of a type *AR* transfer function is smaller than the resonance frequency; i.e., the zero pair, located on the imaginary axis is closer to the origin than the pole pair.

B. Type D: Double Integrator

The type *D* transfer function is given by (1) with $\omega_{\rm ar} = \omega_{\rm r}$, such that it can be rewritten as

$$P_D(s) = \frac{1}{ms^2}. \quad (2)$$

It seems that we have to do with a second-order transfer function that physically is related to a mass with an applied force. However, the denominator polynomial is of second order because the numerator polynomial apparently has two roots that are identical to two roots of the denominator polynomial, i.e., pole–zero cancellation. This can be clearly seen in the pole–zero map of Fig. 1(b).

C. Type RA: Resonance–Antiresonance

This type is comparable to the type *AR* transfer function, but differs because for the type *RA* system the resonance frequency is smaller than the antiresonance frequency. The transfer function of a type *RA* is

$$P_{\rm RA}(s) = \frac{1}{ms^2} \cdot \frac{s^2 + {\omega_{\rm ar}}^2}{s^2 + {\omega_{\rm r}}^2} \cdot \frac{{\omega_{\rm r}}^2}{{\omega_{\rm ar}}^2}, \qquad \omega_{\rm ar} > \omega_{\rm r}. \quad (3)$$

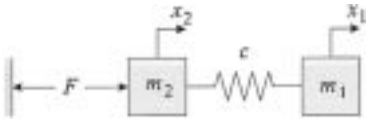

Fig. 2. Flexible mechanism.

The pole–zero map is also shown in Fig. 1(c).

D. Type R: Resonance

The type *R* transfer function is

$$P_R(s) = \frac{1}{ms^2} \cdot \frac{\omega_{\rm r}^2}{s^2 + \omega_{\rm r}^2}. \quad (4)$$

This transfer function type has no zero pair, or rather a zero pair at a frequency outside the frequency range of interest and thus no antiresonance frequency [refer Fig. 1(d)].

E. Type N: Nonminimum Phase

The transfer function of a type *N* system is

$$P_N(s) = \frac{1}{ms^2} \cdot \frac{s^2 - {\omega_{\rm ar}}^2}{s^2 + {\omega_{\rm r}}^2} \cdot \frac{{\omega_{\rm r}}^2}{-{\omega_{\rm ar}}^2}. \quad (5)$$

This type is characterized by a zero at $s = \pm\omega_{\rm ar}$. Because of the zero in the right-half plane [Fig. 1(e)] this type is referred to as nonminimum phase.

III. Classes of Electromechanical Motion Systems

The basic transfer functions listed above describe the dynamic behavior of four *classes* of electromechanical motion systems [6]. These classes are characterized by the mechanical subsystem that contains the dominant stiffness; they are typically obtained after simplification and reduction of more extensive plant models [8]. Per class, we will indicate which basic transfer function type results from a particular position sensor location. Note that an analogous relation between class, velocity sensor location and type exists, however, with only one s less in the denominator of the type.

A. Flexible Mechanism

When the dominant stiffness c is located in the mechanism, the mass-spring-mass model of Fig. 2 can describe the system. This model has been studied extensively [1], [2].

The input force ($u = F$) acts on the motor mass m_2 at position x_2. The position of the end-effector mass m_1 is x_1, which is also the position to be controlled z. When we measure the position of the actuator ($y = x_2$), we obtain a transfer function

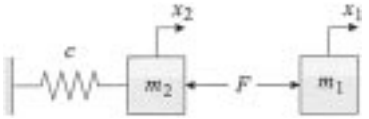

Fig. 3. Flexible frame.

of type *AR*. The parameters in this transfer function are the total mass m, the antiresonance frequency $\omega_{\rm ar}$ and the resonance frequency $\omega_{\rm r}$. The expressions for these parameters, in case of a flexible mechanism, are

$$m = m_1 + m_2 \tag{6}$$

$$\omega_{\rm ar} = \sqrt{\frac{c}{m_1}} \tag{7}$$

$$\omega_{\rm r} = \sqrt{\frac{c}{m_1} + \frac{c}{m_2}}. \tag{8}$$

The transfer function from the input force to the position of the end effector ($y = x_1$) is of type *R*. The expressions for the relevant parameters are as in (6) and (8).

B. Flexible Frame

The model of Fig. 3 describes the situation where the dominant stiffness c is located in the supporting frame. The mass of the frame is m_2 at position x_2. The mass m_1 is a rigid body containing, amongst others, the mass of the actuator and the end effector. The position of this rigid body x_1 is the position to be controlled z. This position can be measured with respect to the frame or with respect to the fixed world, resulting in a different type of transfer function.

The transfer function from the input force ($u = F$) to the position measurement with respect to the frame ($y = x_1 - x_2$) is of type *AR*. The expression for the parameters m, $\omega_{\rm ar}$, and $\omega_{\rm r}$ of the type *AR* transfer function, in case of the flexible frame, are

$$m = m_1 \tag{9}$$

$$\omega_{\rm ar} = \sqrt{\frac{c}{m_1 + m_2}} \tag{10}$$

$$\omega_{\rm r} = \sqrt{\frac{c}{m_2}}. \tag{11}$$

When the end-effector position is measured with respect to the fixed world ($y = x_1$), we obtain a transfer function of type *D*. The single parameter in this transfer function is m (9). The resonance frequency $\omega_{\rm r}$ is cancelled by an antiresonance frequency $\omega_{\rm ar}$ of equal magnitude, according (11).

C. Flexible Actuator Suspension

The model of Fig. 4 represents a system consisting of a rotating actuator with transmission that is contained in a flexible linear suspension (refer to the Appendix).

Linear movements of the end effector m_1 are a combination of movements due to actuator rotations and suspension vibrations. The actuator, with an applied torque T, has an inertia J. Together with the rotation-to-translation transmission i m it is placed in a suspension with mass m_2 and stiffness c. The linear velocity of the end effector m_1 is the addition of the velocity

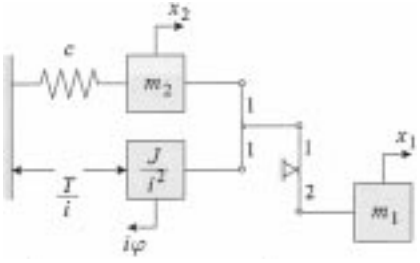

Fig. 4. Flexible suspension.

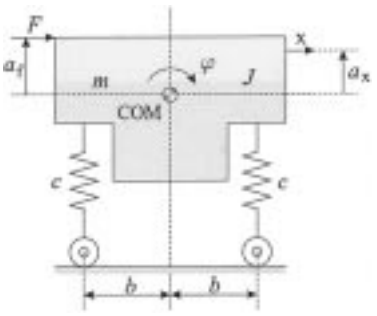

Fig. 5. Flexible guidance.

of the suspension and the transformed angular velocity of the actuator. In Fig. 4, this is represented by the combination of transmissions between the masses. The figure also shows how the torque T, the actuator position φ and the actuator inertia J have been transformed. The transfer function from the input force ($u = T/i$) to the position of the actuator ($y = i\varphi$) is of type *AR*. The expressions for parameters in the type *AR* transfer function of the flexible actuator suspension are

$$m = \frac{J}{i^2} + m_1 \tag{12}$$

$$\omega_{\rm ar} = \sqrt{\frac{c}{m_1 + m_2}} \tag{13}$$

$$\omega_{\rm r} = \sqrt{\frac{(J + i^2 m_1)c}{J(m_1 + m_2) + i^2 m_1 m_2}}. \tag{14}$$

When the position of the end effector is measured ($y = x_1$), a type *RA* transfer function is obtained. The expression for the antiresonance frequency is

$$\omega_{\rm ar} = \sqrt{\frac{c}{m_2}}. \tag{15}$$

In [4], a physical interpretation of transfer function zeros for simple control systems with mechanical flexibilities is given. It is shown that whereas the poles are the resonances of a flexible structure, the zeros are the resonances of a constrained substructure. In case of the flexible mechanism, flexible frame and flexible suspension, the antiresonance frequency can be looked upon as the resonance frequency of the system in case the actuator is blocked, i.e., constrained.

D. Flexible Guidance

The final class is characterized by flexibility in the guiding system. In Fig. 5, the dynamics of this class are illustrated. Due

to an input force ($u = F$) the mass m will move in the x direction. Additionally, F will excite a rocking mode around the center of mass (COM), due to flexibilities c.

The type of transfer function from the input force ($u = F$) to the measured position ($y = x$) depends on geometrical properties: the distances a_{f} and a_{x}. The expressions for parameters in the transfer function are

$$\omega_{\mathrm{ar}} = \sqrt{\frac{k}{J + m a_{\mathrm{f}} a_{\mathrm{x}}}} \tag{16}$$

$$\omega_{\mathrm{r}} = \sqrt{\frac{k}{J}} \tag{17}$$

where,

$$k = 2cb^2. \tag{18}$$

We can distinguish five situations:

1) When F and x are on the same side of the COM ($a_{\mathrm{x}} > 0$ and $a_{\mathrm{f}} > 0$ or $a_{\mathrm{x}} < 0$ and $a_{\mathrm{f}} < 0$) we obtain a type *AR* transfer function, because $\omega_{\mathrm{ar}} < \omega_{\mathrm{r}}$;
2) When either F or x are exactly located at the COM ($a_{\mathrm{x}} = 0$ or $a_{\mathrm{f}} = 0$), we obtain a type D transfer function, as $\omega_{\mathrm{ar}} = \omega_{\mathrm{r}}$. Note that $a_{\mathrm{x}} = 0$ or $a_{\mathrm{f}} = 0$ are two different situations, where the plant is unobservable respectively uncontrollable;
3) When F and x are on different sides of the COM ($a_{\mathrm{x}} > 0$ and $a_{\mathrm{f}} < 0$) or ($a_{\mathrm{x}} < 0$ and $a_{\mathrm{f}} > 0$) we obtain a type *RA* transfer function, under the condition that $J + m a_{\mathrm{x}} a_{\mathrm{f}} > 0$;
4) When F and x are on different sides of the COM and $J + m a_{\mathrm{x}} a_{\mathrm{f}} \approx 0$ we obtain an R type transfer function, as ω_{ar} is located at infinity; and
5) When F and x are on different sides of the COM and $J + m a_{\mathrm{x}} a_{\mathrm{f}} < 0$ we obtain an N type transfer function, as ω_{ar} is complex.

IV. Controlled Plant Dynamics

In [9] as well as in [6] design knowledge has been formalized for the design of electromechanical transient systems, in case the dominant stiffness is located in the mechanism, i.e., Fig. 2. A design procedure has been formulated that aims for the minimization of the positional error of the end effector after a change in the reference path (point-to-point motion). We will extend this method such that it is applicable to all classes of electromechanical motion systems presented in the previous section.

A. Closed-Loop Characteristics

Before we can consider the closed-loop transfer, we have to make a choice for the control system. We have chosen a proportional differential (PD)-type control system that implements a proportional action k_{p} on a positional error and a proportional action k_{d} on a measured (or estimated) velocity ν (Fig. 6). The positional error is obtained as the difference between a measured position y and the reference path r. The variable to be controlled is the position of the end effector z. Our choice for this

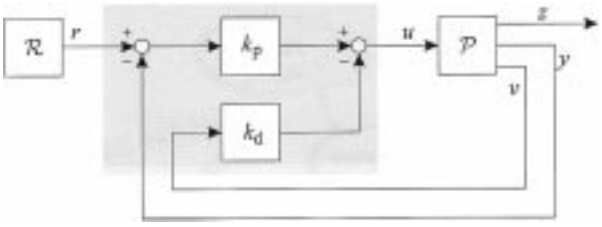

Fig. 6. General closed-loop transient system.

controller structure is basically motivated by the fact that now a fair tradeoff can be made between influence of controller factors versus plant factors on system performance. Furthermore, if one would allow for a higher order controller, one unjustly presumes to have perfect knowledge about all relevant plant properties; unrealistically optimistic predictions of achievable system performance would result then in general.

We now introduce a number of (dimensionless) quantities that allow us to draw general conclusions for controlled fourth-order systems. First we define two loop quantities: the position loop quantity ω_{p} and the velocity loop quantity ω_{d}

$$\omega_{\mathrm{p}} = \sqrt{\frac{k_{\mathrm{p}}}{m}} \tag{19}$$

$$\omega_{\mathrm{d}} = \frac{k_{\mathrm{d}}}{m}. \tag{20}$$

An important dimensionless quantity, which is related to the plant is the frequency ratio ρ

$$\rho = \left(\frac{\omega_{\mathrm{ar}}}{\omega_{\mathrm{r}}}\right)^2. \tag{21}$$

This ratio relates the resonance frequency[1] of a plant to the antiresonance frequency.

The dimensionless controller settings Ω_{p} and Ω_{p} relate the loop quantities ω_{p} and ω_{d} to the antiresonance frequency of the plant. These settings are the dimensionless versions of the proportional actions k_{p} and k_{d}.

$$\omega_{\mathrm{p}} = \Omega_{\mathrm{p}} \cdot \omega_{\mathrm{ar}} \tag{22}$$

$$\omega_{\mathrm{d}} = \Omega_{\mathrm{d}} \cdot \omega_{\mathrm{ar}}. \tag{23}$$

The reference path is assumed to be a smooth spline function. The smoothness is determined by a degree. A reference path of degree two involves two pieces of second-order polynomials. The reference path specifies, in terms of the position of the end effector, a distance h_{m} that has to be covered within a motion time t_{m}. The control goal is to guarantee an upper bound e_0 on the absolute value of the positional error of the end effector after the reference path has reached the end point (Fig. 7).

The maximal relative positional error E_0 is defined as the ratio between the positional error e_0 and the motion distance h_{m}

$$E_o = \frac{e_o}{h_{\mathrm{m}}}. \tag{24}$$

[1]For type *R*, the frequency ratio generally reduces to a mass ratio. For example, for the flexible mechanism class with a type *R* transfer $\rho = \frac{m2}{m}$.

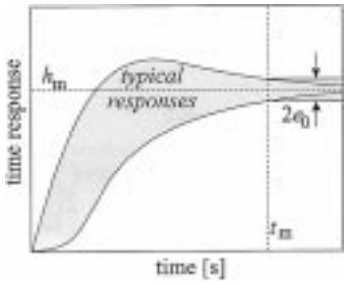

Fig. 7. Reference path and typical response.

A crucial dimensionless quantity is the periodic ratio τ that relates the antiresonance frequency of the plant and the motion time t_{m}

$$\tau = \frac{2\pi}{\omega_{\mathrm{ar}} t_{\mathrm{m}}}. \tag{25}$$

B. Closed-Loop Transfer Functions

We now consider the closed-loop transfer functions $H(s)$,i.e., the transfer functions from the reference path r to the measured position y, when using a control system as in Fig. 6. In this configuration, two measurements are needed and hence several sensor combinations can be thought of for each class, depending on the location and the reference of the position and velocity measurement. For example, for the flexible transmission class, three combinations can be made:

1) position and velocity measurement at the actuator;
2) position and velocity measurement at the end effector;
3) position measurement at the end effector and velocity measurement at the actuator.

In Section III, it has been shown how a class and a sensor location and reference together determine a type. Hence, we can categorize all relevant closed loop transfer functions on basis of the two types that describe the position and velocity plant transfer. Furthermore, the dimensionless quantities described above can be used to characterize these closed-loop dynamics in general terms, independent of a particular class. We will refer to the various forms of closed-loop transfer functions as *concepts* and indicate a particular concept by listing the (two) types, where the velocity transfer type is listed first.

As an example we consider the flexible mechanism. When both the actuator position and velocity are measured, both the open-loop transfer functions, from input force F to the measured position y and to the measured velocity ν, are characterized by a type *AR* and we obtain concept *AR–AR*, or concept *AR* for short. The corresponding closed-loop transfer function $H(s)$ can be expressed in terms of the dimensionless quantities

$$H_{\mathrm{AR}}(s) = \frac{b_2 s^2 + b_1 s + b_0}{a_4 s^4 + a_3 s^3 + a_2 s^2 + a_1 s + a_0} \tag{26}$$

where

$$\begin{array}{ll} b_2 = \omega_{\mathrm{p}}^2 \omega_{\mathrm{r}}^2 & a_4 = \omega_{\mathrm{ar}}^2 \\ b_1 = 0 & a_3 = \omega_{\mathrm{d}} \omega_{\mathrm{r}}^2 \\ b_0 = \omega_{\mathrm{ar}}^2 \omega_{\mathrm{p}}^2 \omega_{\mathrm{r}}^2 & a_2 = \left(\omega_{\mathrm{ar}}^2 + \omega_{\mathrm{p}}^2\right) \omega_{\mathrm{r}}^2 . \\ & a_1 = \omega_{\mathrm{d}} \omega_{\mathrm{ar}}^2 \omega_{\mathrm{r}}^2 \\ & a_0 = \omega_{\mathrm{ar}}^2 \omega_{\mathrm{p}}^2 \omega_{\mathrm{r}}^2 \end{array} \tag{27}$$

When, for example, we measure the actuator velocity and end-effector position of the flexible mechanism, the open-loop transfer function from the input force F to the measured position y is of type R and from the input force F to the measured velocity ν is of type *AR*. We now obtain concept *AR–R*. We can also describe this closed-loop transfer function $H(s)$ in terms of dimensionless quantities

$$H_{\mathrm{AR-R}}(s) = \frac{b_0}{a_4 s^4 + a_3 s^3 + a_2 s^2 + a_1 s + a_0}. \tag{28}$$

The coefficients in this function are

$$\begin{array}{lll} b_0 = \omega_{\mathrm{ar}}^2 \omega_{\mathrm{p}}^2 \omega_{\mathrm{r}}^2 & a_4 = \omega_{\mathrm{ar}}^2 \\ & a_3 = \omega_{\mathrm{d}} \omega_{\mathrm{r}}^2 \\ & a_2 = \omega_{\mathrm{r}}^2 \omega_{\mathrm{ar}}^2 \\ & a_1 = \omega_{\mathrm{d}} \omega_{\mathrm{ar}}^2 \omega_{\mathrm{r}}^2 \\ & a_0 = \omega_{\mathrm{ar}}^2 \omega_{\mathrm{p}}^2 \omega_{\mathrm{r}}^2 . \end{array} \tag{29}$$

In [10] the transfer functions for all relevant concepts have been derived. So far, the transfer functions have been described without mechanical damping, as damping is not of importance for conceptual design of the controlled system. However, during the simulations in the next section we will implicitly use a small amount of damping [10].

V. Choosing Design Parameters

A. Dimensionless Optimal Controller Settings

The dimensionless closed-loop transfer functions $H(s)$ of the concepts defined above relate design factors of the plant and the controller to system performance. Different values for the dimensionless controller settings Ω_{p} and Ω_{d} result in different values for the loop quantities ω_{p} and ω_{d} and thus in different closed-loop transfer functions $H(s)$. This is explored by performing numerous simulations with these transfer functions for various *controller settings* and identical reference paths and the positional error is determined. Feasible dimensionless controller settings are defined as those values that result in a small enough positional error with a sufficient stability margin [9]. The dimensionless version of this margin is defined as

$$G = \frac{g}{\omega_{\mathrm{ar}}}. \tag{30}$$

A sufficient stability margin is considered to be attained for $G = 0.2$. So the stability margin defines a forbidden region between $-g$ and 0 in the s plane, for the poles of the closed-loop system $H(s)$. When we determine the feasible dimensionless controller settings, we implicitly assume that the settings that lead to a minimal error of the measured position y also lead to a minimal error of the end-effector position z.

The *optimal dimensionless controller settings* are defined as those settings that result in the smallest positional error with a sufficient stability margin, for different values of the *frequency ratio* ρ.

In Fig. 8 three charts are shown for concept *AR* with feasible regions for different frequency ratios. These regions indicate values of Ω_{p} and Ω_{d} that result in a relative positional error E_0 smaller than 0.01, 0.02, 0.04, and 0.08, while meeting

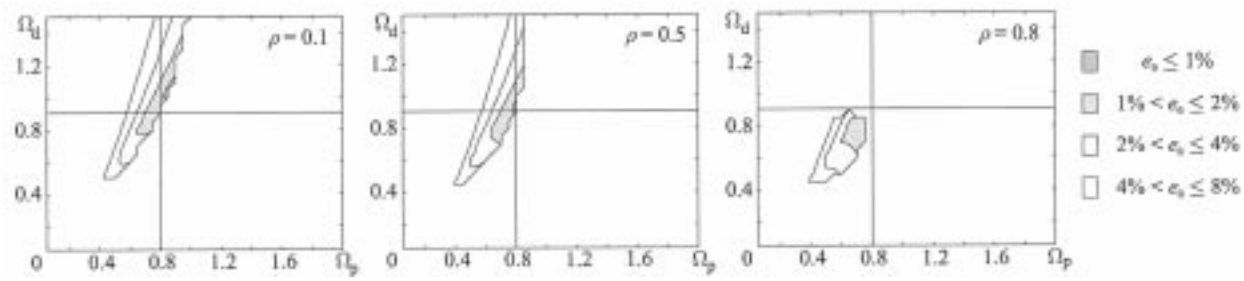

Fig. 8. Regions with feasible dimensionless controller settings for concept *AR*.

TABLE I
OPTIMAL DIMENSIONLESS CONTROLLER SETTINGS

Concept	Condition	Optimal	
		Ω_p	Ω_d
AR	$0.1 < \rho < 0.8$	0.8	0.9
D	-	0.9	0.9
RA	-	-	-
R	$0.1 < \rho < 0.12$	1.4	0.45
N	-	-	-
AR-D	$0.1 < \rho < 0.75$	0.7	0.7
AR-RA	$0.1 < \rho < 0.8$ $1.0 < \rho^* < 1.4$	0.6	0.6
AR-R	$0.1 < \rho < 0.5$	0.6	0.7
AR-N	$0.1 < \rho < 0.5$ $0.5 < \rho^* < 1.4$	0.5	0.6

the stability margin (30). The difference between these charts is the value for the frequency ratio ρ that is used: 0.1, 0.5, respectively, 0.8. The values for the (dimensionless) damping used in the simulations are similar as the values used in [9] and reflect practical settings, refer [10]. During all simulations discussed in this section we use a second-degree reference path with a motion time t_m of 1 s and a periodic time constant τ of 0.4.

From these three charts we select the optimal dimensionless controller settings for concept *AR* as $\Omega_p = 0.8$ and $\Omega_d = 0.9$, which are indicated in Fig. 8 by means of a cross hair. The cross hair cannot be located exactly in the regions with minimal error for all values for the frequency ratio ρ; rather an acceptable location as close as possible to these regions has been selected.

Not for all concepts feasible dimensionless controller settings can be determined, as some transfer function types, e.g., type *RA*, cannot be stabilized by means of a PD-type controller as in Fig. 6. Table I indicates the optimal dimensionless controller settings for all concepts and gives limitations on the values of the frequency ratio ρ for which these settings are applicable. The ratio ρ^* indicates a frequency ratio, according (21), with an antiresonance frequency that is *larger* than the resonance frequency. This antiresonance frequency generally occurs in the transfer function from input force to end-effector position.

B. Dimensionless Problem-Plant Relation

Using the dimensionless quantities and the optimal dimensionless controller settings, we can determine a relation between the specification, i.e., the desired motion of the end effector and the plant, which is independent of the particular problem setting. This relation is expressed in terms of the maximum relative positional error E_0 and the periodic ratio τ. We consider the dimensionless closed-loop transfer functions, i.e., the concepts described in the previous section, with the optimal dimensionless quantities of Table I. In numerous simulations the periodic ratio τ is varied, by applying different second-degree reference paths to the (optimal) closed-loop transfer functions. For all values of τ the relative positional error is calculated. The upper bound for second-degree reference paths can be expressed as [9]

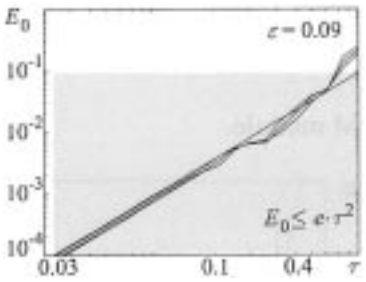

Fig. 9. Relative positional error as a function of the periodic ratio τ for concept *AR* and second-degree reference paths, using $\rho = 0.1, 0.5$, and 0.8.

$$E_0 = \varepsilon \cdot \tau^2 \tag{31}$$

where ε is a constant that depends on the particular concept that is considered. We mainly considered the situations where the relative positional error is smaller than 1%, as this is generally required by modern electromechanical motion systems.

As an example, the relation between the relative positional error E_0 and the periodic ratio τ for concept *AR* is calculated for three different values of the frequency ratio ρ: 0.1, 0.5, and 0.8. During all simulations discussed in this section we use an antiresonance frequency ω_{ar} of 1 rad/s. In Fig. 9, the results of the simulations with a second-degree reference path are shown. The straight line indicates the estimated upper bound of the positional error. For $\tau < 0.4$ the constant ε in the expression for the upper bound (31) for concept *AR* equals 0.09.

Instead of using a second-degree reference path, the designer may choose a third-degree reference path, i.e., a reference path with limited jerk. When the same simulations as above are performed, an upper bound for third-degree reference paths can also be determined. The upper bound is characterized by

$$E_0 = \gamma \cdot \tau^3. \tag{32}$$

TABLE II
DIMENSIONLESS PROBLEM-PLANT RELATIONS

Concept	Condition	Performance ε	Performance γ
AR	$0.1 < \rho < 0.8$	0.09	0.35
D	-	0.07	0.21
R	$0.1 < \rho < 0.12$	0.06	0.06
AR-D	$0.1 < \rho < 0.75$	0.11	0.33
AR-RA	$0.1 < \rho < 0.8$ $1.0 < \rho^* < 1.4$	0.17	0.60
AR-R	$0.1 < \rho < 0.5$	0.12	0.40
AR-N	$0.1 < \rho < 0.5$ $0.5 < \rho^* < 1.4$	0.22	0.60

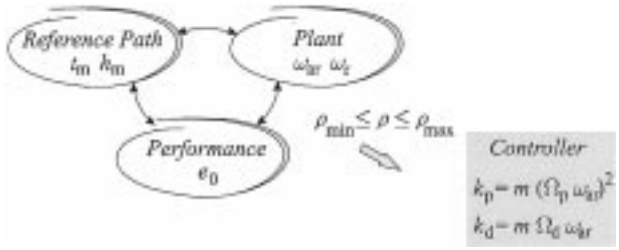

Fig. 10. Application of assessment method.

In Table II the dimensionless problem-plant relations for all feasible concepts are summarized (refer [10]) for both second- and third-degree reference paths.

VI. ASSESSMENT PROCEDURE

So far, we have determined (dimensionless) relations between the attainable performance, the reference path and the plant, which are independent of the particular problem setting.

Together with the optimal dimensionless controller settings, we use these relations to formulate an assessment method that can be used in various ways, depending upon the specific design context. The three crucial design parameters are the periodic ratio τ, the antiresonance frequency ω_{ar} and the relative servo error E_0. Once two of these three design parameters are chosen, the third will follow automatically. If the frequency ratio ρ lies between its lower and upper bound given in Table I, the optimal controller settings can be found, such that the controlled system fulfills all specifications. This is visualized in Fig. 10. The assessment procedure consists of the following steps.

1) Determine the class of electromechanical motion systems that is at hand and the type of plant transfer function. Calculate ω_{ar}, ω_{r}, and ρ.
2) Determine the concept that is at hand, by looking at the location of the position and velocity sensor. Refer to Table I to verify whether optimal dimensionless controller settings can validly be applied.
3) Depending on the situation perform one of the following three alternatives.
   a) When the reference path and the desired performance are fixed, calculate the periodic ratio τ, using Table II and
   $$\tau = \sqrt{\frac{E_o}{\varepsilon}} \text{ or } \tau = \sqrt[3]{\frac{E_o}{\gamma}}.$$
   Determine the minimal required antiresonance frequency of the plant with
   $$\omega_{\mathrm{ar,req}} = \frac{2\pi}{\tau t_{\mathrm{m}}}.$$
   This value can be used to calculate the required (dominant) stiffness of a particular plant, as well as the resonance frequency ω_{r}, in case the mass distribution is assumed to be fixed.
   b) When the reference path and the antiresonance frequency of the plant are known, calculate τ according
   $$\tau = \frac{2\pi}{\omega_{\mathrm{ar}} t_{\mathrm{m}}}$$
   and determine the attainable performance, using Table II and
   $$E_0 = \varepsilon \cdot \tau^2 \text{ or } E_0 = \gamma \cdot \tau^3.$$
   c) When the desired performance and the antiresonance frequency of the plant are known, calculate τ as a function of the motion distance h_{m} using Table II and
   $$\tau = \sqrt{\frac{e_0}{\varepsilon \cdot h_{\mathrm{m}}}} \text{ or } \tau = \sqrt[3]{\frac{e_0}{\gamma \cdot h_{\mathrm{m}}}}.$$
   Next, determine the reference path, by finding a tradeoff between the motion distance h_{m} and the motion time t_{m} that fulfills the equality
   $$\sqrt{\frac{e_0}{\varepsilon \cdot h_{\mathrm{m}}}} = \frac{2\pi}{\omega_{\mathrm{ar}} t_{\mathrm{m}}}.$$
4) When the frequency ratio ρ fulfills the requirements of Table I, the control system for a particular problem setting and a particular controller configuration can be implemented by
   $$k_{\mathrm{p}} = m \cdot (\Omega_{\mathrm{p}} \cdot \omega_{\mathrm{ar}})^2 \text{ and } k_{\mathrm{d}} = m \cdot \Omega_{\mathrm{d}} \cdot \omega_{\mathrm{ar}}.$$

VII. APPLICATION TO AN INDUSTRIAL MOTION SYSTEM

We have developed the assessment method for application in a mechatronic design process, where a realization of the complete electromechanical subsystem is not existing during the design of the control system. However, the actual design of other subsystems than the control system is out of the scope of this paper. Therefore, we will use an existing Placement Module (Fig. 11) of the Philips Fast Component Mounter (FCM), as an example of an industrial electromechanical motion system, to

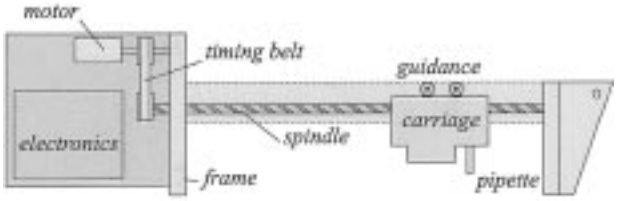

Fig. 11. Placement module of the FCM.

TABLE III
SPECIFICATIONS FOR THE PM MODULE

quantity		value
maximum error	e_0	100 [μm]
motion time	t_m	250 [ms]
motion distance	h_m	0.15 [m]
settling time	t_s	30 [ms]
maximum acceleration	a_{max}	10
maximum velocity	v_{max}	1

evaluate and to illustrate the assessment method. It is not an objective to maximize the performance of this specific PM module, using detailed knowledge of the plant dynamics obtained from system identification. Rather, our aim is to satisfy the requirements in a short design cycle. We will only use that plant knowledge that generally would have been available at the conceptual design stage. The resulting control system will be applied without additional tuning, in order to get a fair impression on the practical relevance.

A. Characterization of the Task

The task of the PM module is to place a component with an accuracy of 100 μm at 30 ms after the motion time. The maximum velocity and acceleration of the system are specified as 1 [$m \cdot s^{-1}$], respectively, 10 [$m \cdot s^{-2}$] [11]. We consider a 1-D motion along the spindle, i.e., in y direction. The relation between the motion distance h_m, the motion time t_m, maximum acceleration a_{max} and maximum velocity ν_{max} for the prescribed second-degree path is [6]

$$\left.\begin{aligned} a_{max} &= 4\frac{h_m}{t_m^2} = 10\,[m \cdot s^{-2}] \\ \nu_{max} &= 2\frac{h_m}{t_m} = 1.0\,[m \cdot s^{-2}] \end{aligned}\right\} \Rightarrow \begin{aligned} h_m &= 0.1\ m \\ t_m &= 0.2\ s \end{aligned}. \quad (33)$$

This is the characteristic task of the controlled system, i.e., the performance obtained for this task is characteristic for the controlled system. The task we will use in simulations and experiments will also include a period of 0.05 s with constant maximum velocity. We will use the task specified in Table III.

B. Characterization of the Plant Dynamics

We start with a simple model of the PM module that is built from several component models. In Fig. 12, the initial bond graph model of the PM module is shown.

The component models are described in [10], as are the results of simplification and order reduction. The outcome is shown as the fourth-order model in Fig. 13 .

The values for the physical parameters in this model are shown in Table IV.

Fig. 12. Initial bond graph model of the PM module.

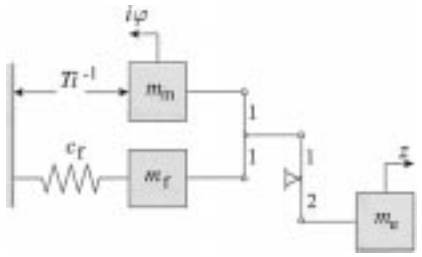

Fig. 13. Fourth-order model of the PM module.

TABLE IV
PHYSICAL PARAMETER VALUES IN MODEL OF PM MODULE

quantity		value
motor mass	m_m	6.53 [kg]
frame stiffness	c_f	$4.3 \cdot 10^6$
frame mass	m_f	11.5 + 5 [kg]
end-effector	m_e	2.3 [kg]

C. Performance Assessment

Once the plant model is in the standard form, we apply the assessment method.

1) Determine the class of electromechanical motion system that is at hand. In Fig. 13 we recognize the flexible actuator suspension (refer Section II). We consider the transfer functions from the input force Ti^{-1} to the actuator position $i\varphi$ and to the end-effector position z. The total mass to be moved equals

$$m = m_m + m_e = 8.83\ kg. \quad (34)$$

When the actuator position is considered the transfer function is of type *AR*. The antiresonance frequency, respectively, resonance frequency of the lowest mode of vibration is

$$\omega_{ar} = \sqrt{\frac{c}{m_f + m_e}} = 478\ \frac{rad}{s} \quad (35)$$

$$\omega_r = \sqrt{\frac{c(m_m + m_e)}{m_m(m_f + m_e) + m_f m_e}} = 486\ \frac{rad}{s}. \quad (36)$$

When the end-effector position is considered, we obtain a type *RA* transfer function, with antiresonance frequency

$$\omega_{ar} = \sqrt{\frac{c_f}{m_f}} = 510\ \frac{rad}{s}. \quad (37)$$

2) Determine the concept that is at hand, by looking at the location of the position and velocity sensor. Refer to Table I

to verify whether optimal dimensionless controller settings can validly be applied. In the case of the PM there are three possible concepts:

a) Concept *AR*: position and velocity measurement at the actuator;

b) Concept *RA*: position and velocity measurement at the end effector;

c) Concept *AR–RA*: position measurement at the end effector and velocity at the actuator.

The actual PM module only contains a position sensor on the motor axis, therefore, we will consider concept *AR*. Whether the optimal dimensionless controller settings can validly be applied depends on the value of the frequency ratio ρ. For concept *AR*, the frequency ratio must have a value between 0.1 and 0.8. The actual value of the frequency ratio is

$$\rho = \left(\frac{\omega_{\mathrm{ar}}}{\omega_{\mathrm{r}}}\right)^2 = 0.97 \tag{38}$$

which is larger than the permitted 0.8. Despite this fact, we will continue application of the assessment method, but we have to reconsider the violation of the bounds on ρ afterwards,

3) Depending on the situation, perform one of three alternatives.

a) When we assume the reference path and the desired performance, in terms of the maximal positional error e_0, to be fixed, we calculate the periodic ratio τ according

$$\tau = \sqrt{\frac{e_0}{\varepsilon \cdot h_{\mathrm{m}}}} = \sqrt{\frac{1.0 \cdot 10^{-4}}{0.09 \cdot 0.1}} = 0.11. \tag{39}$$

Here, we selected the value for ε from Table II. The minimal required antiresonance frequency of the plant is

$$\omega_{\mathrm{ar,req}} = \frac{2\pi}{\tau t_{\mathrm{m}}} = \frac{2\pi}{0.11 \cdot 0.2} = 298\ \frac{\mathrm{rad}}{\mathrm{s}} \tag{40}$$

which is smaller than the actual antiresonance frequency, thus the lowest mode of vibration is not an unacceptable limitation for the desired performance;

b) When we assume the reference path and the antiresonance frequency to be fixed, we calculate the periodic ratio τ according

$$\tau = \frac{2\pi}{\omega_{\mathrm{ar}} t_{\mathrm{m}}} = 0.066. \tag{41}$$

The attainable performance in this situation is predicted as

$$e_0 = E_0 \cdot h_{\mathrm{m}} = \varepsilon \cdot \tau^2 \cdot h_{\mathrm{m}} = 39\ \mu\mathrm{m} \tag{42}$$

which is smaller than the desired accuracy of 100 μm;

c) When we assume the desired performance and the antiresonance frequency to be fixed, we can propose a characteristic reference path. This requires a tradeoff between the motion time and the motion distance

$$\begin{aligned} \frac{2\pi}{\omega_{\mathrm{ar}} t_{\mathrm{m}}} &= \sqrt{\frac{e_0}{\varepsilon \cdot h_{\mathrm{m}}}} \\ \Rightarrow t_{\mathrm{m}}^2 &= 0.16 \cdot h_{\mathrm{m}}. \end{aligned} \tag{43}$$

4) Determine the control system for a particular problem setting. The dimensionless optimal controller settings for concept *AR* are $\Omega_{\mathrm{p}} = 0.8$ and $\Omega_{\mathrm{d}} = 0.9$ (refer to Table I). For the particular problem setting of the PM module, with $\omega_{\mathrm{ar}} = 478$ rad/s, we obtain

$$\begin{aligned} k_{\mathrm{p}} &= m \cdot (\Omega_{\mathrm{p}} \cdot \omega_{\mathrm{ar}})^2 = 1.29 \cdot 10^6 \\ k_{\mathrm{d}} &= m \cdot \Omega_{\mathrm{d}} \cdot \omega_{\mathrm{ar}} = 3.80 \cdot 10^3. \end{aligned} \tag{44}$$

From application of the assessment method we learn that the specifications can be met with the given electromechanical subsystem. The specification given for the PM module requires the positional error to be attained only after a settling time of 30 ms. After this settling time the maximum positional error will only have decreased further. As the frequency ratio (38) of the PM module is not within the bounds specified by the assessment method, the stability margin may be smaller than guaranteed. The guaranteed margin is such that the closed-loop poles are located sufficiently far, i.e., a distance $-g$, into the left-half plane. For the PM module the required margin is

$$g = G \cdot \omega_{\mathrm{ar}} = 96. \tag{45}$$

The actual margin, with damping as used in the assessment method is significantly smaller: only 41. However, a type *AR* transfer function with a PD-type controller is always stable, therefore, we will proceed with the design, with the knowledge that the stability margin may require extra attention in the remainder of the design process.

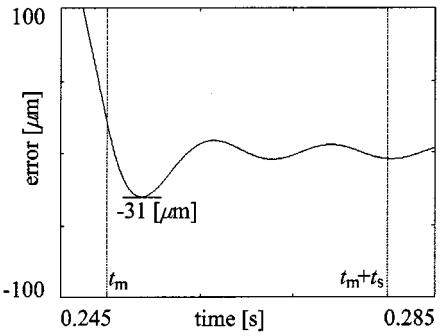

Fig. 14. Simulation of the positional error at the end effector, with fourth-order plant model.

D. Simulation Experiments

The simulations show that the positional error after the motion time t_{m} is 31 μm (Fig. 14), which is indeed smaller than the predicted maximum positional error of 39 μm. After the settling time t_{s} of 30 ms, we see that the error has decreased even further. Therefore, we conclude that we obtained a feasible design for the controlled system and one could continue the design process, keeping in mind the relatively small stability margin.

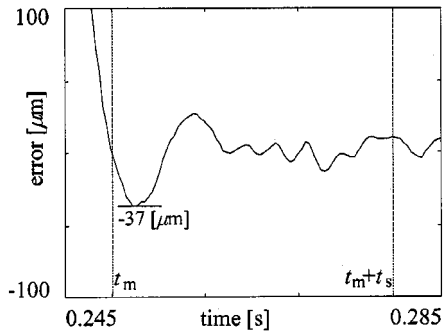

Fig. 15. Measurement with PSD at pipette.

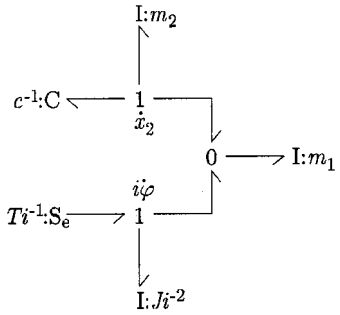

Fig. 16. Bond graph of flexible actuator suspension.

E. Practical Experiments

We have applied and tested the controller to the real PM module. The motor position is measured by an encoder that can measure 2000 steps per revolution, which corresponds to a resolution of 10 μm at the end effector. The position of the end effector is measured over a small range by means of a position sensitive detector (PSD), such that we can verify the behavior of the variable of interest. The PSD output is not used for feedback.

The maximal positional error after the motion time is 37 μm (Fig. 15), which is 6 μm larger than in simulation, but corresponding well with the positional error of 39 μm predicted by the assessment method.

VIII. Conclusion

The aim of conceptual design is to obtain a feasible design for the path generator, control system and electromechanical plant with appropriate sensor locations, in an integrated way. For transient systems, i.e., positioning systems, this has been worked out.

First we described standard problems, by means of a classification of four electromechanical motion systems. These *classes* use standard fourth-order plant transfer functions, which are referred to as *types*. Dimensionless quantities are used to characterize closed-loop behavior, i.e., reference path generator, controller and plant. Again several standard closed-loop transfer functions have been defined, which are referred to as *concepts*.

For these standard problems we have determined standard solutions. Relations between the dimensionless quantities of the reference path, controller and plant have been obtained heuristically by means of numerous simulations. These relations can now be used in an *assessment method*, which considers functional interaction between domain specific subsystems.

By means of application to an industrial motion system, we have illustrated the design enhancement presented in this paper. We mainly focussed on evaluation of the design enhancement and not on maximization of the performance of the controlled system. Assessment learned that the specification of a maximal positional error of 100 μm can be met; a maximal error of 39 μm was indicated as feasible. Simulations with an initial plant model, as well as practical experiments, confirmed these results. This illustrates that, using minimal plant knowledge, the assessment method provides the designer with relevant knowledge about the design problem, early in the design process.

The principal benefits of the assessment method are that it can quickly provide insight in the design problem and that feasible goals and required design efforts can be estimated at an early stage.

Appendix
Flexible Actuator Suspension

In order to clarify the iconic diagram of Fig. 4, we show a bond graph model of the flexible actuator suspension in Fig. 16.

Here, it can be seen that the construction of transformers in Fig. 4 corresponds to a 0-junction. Thus the velocity of the end effector is a summation of the velocity of the rotating actuator–transmission combination and the velocity of the flexible suspension.

References

[1] M. Steinbuch and M. L. Norg, "Advanced motion control: An industrial perspective," *Eur. J. Control*, vol. 4, pp. 278–293, 1998.

[2] B. Wie and D. S. Bernstein, "Benchmark problems for robust control design," in *Proc. Amer. Control Conf.*, Boston, MA, 1991, pp. 1929–1930.

[3] B. Armstrong-Hélouvry, P. Dupont, and C. Canudas de Wit, "A survey of models, analysis tools and compensation methods for control of machines with friction," *Automatica*, vol. 30, pp. 1083–1138, 1994.

[4] D. K. Miu, "Physical interpretation of transfer function zeros for simple control systems with mechanical flexibilities," *Trans. ASME, J. Dyn. Syst. Meas. Control*, vol. 113, pp. 419–424, 1991.

[5] ——, *Mechatronics–Electromechanics and Contromechanics*. New York: Springer-Verlag, 1993.

[6] M. P. Koster, W. T. C. van Luenen, and T. J. A. de Vries, *Mechatronica (Mechatronics), in Dutch, course material*. Enschede, The Netherlands: University of Twente, 1999.

[7] A. M. Rankers, "Machine dynamics in mechatronic systems–an engineering approach," Ph.D. dissertation, Univ. Twente, Enschede, The Netherlands, 1997.

[8] J. van Amerongen, E. Coelingh, and T. J. A. de Vries, "Computer support for mechatronic control system design," *J. Robot. Autonomous Syst.*, vol. 30, 2000.

[9] H. Groenhuis, "A design tool for electromechanical servo systems," Ph.D. dissertation, Univ. Twente, Enschede, The Netherlands, 1991.

[10] H. J. Coelingh, "Design support for motion control systems–a mechatronic approach," Ph.D. dissertation, Univ. Twente, Enschede, The Netherlands, [Online]. Available: http://www.ce.utwente.nl/clh/.

[11] Philips, *Fast Component Mounter–II Specifications*. Eindhoven, The Netherlands: Technical Univ. of Eindhoven, 1998.

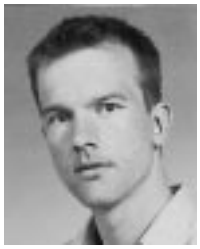

Erik Coelingh (M'98) was born in Hengelo, The Netherlands, in 1971. He received the M.Sc. and the Ph.D. degrees from the Faculty of Electrical Engineering, University of Twente, Enschede, The Netherlands, in 1995 and 2000, respectively.

Currently, he works in vehicle control at the Chassis Department of the Volvo Car Corporation, Gothenburg, Sweden. His research interests include design support for motion control systems using a mechatronic approach.

Theo J. A. de Vries (M'96) was born in Wolvega, The Netherlands, in 1966. He received the M.Sc. and Ph.D. degrees in electrical engineering from the University of Twente, Enschede, The Netherlands, in 1990 and 1994, respectively, following a special program that combined courses of the Faculties of Electrical Engineering and Mechanical Engineering.

From 1994 to 1999, he was an Assistant Professor and since 1999, he has been an Associate Professor in intelligent control and mechatronics at the Control Laboratory, University of Twente. His main research interest is the development of controlled electromechanical systems using learning controllers.

Rien Koster started his professional carreer as a designer of production equipment with Philips Electronics, Amsterdam, The Netherlands, in 1967. In 1985 he became a Professor in mechanical design with the Faculty of Mechanical Engineering at the Technical University of Eindhoven, Eindhoven, The Netherlands. Since 1990, he has been a Professor of mechatronics with both the Faculty of Mechanical Engineering and the Faculty of Electrical Engineering at the University of Twente, Enschede, Netherlands.